



Regulative differentiation as bifurcation of interacting cell population

Akihiko Nakajima^{a,*}, Kunihiko Kaneko^{a,b}

^a Department of Basic Science, University of Tokyo, 3-8-1 Komaba, Meguro-ku, Tokyo 153-8902, Japan

^b ERATO Complex Systems Biology Project, JST, Japan

ARTICLE INFO

Article history:

Received 3 December 2007

Received in revised form

8 April 2008

Accepted 9 April 2008

Available online 16 April 2008

Keywords:

Intercellular coupling

Cell clustering

Functional module

ABSTRACT

In multicellular organisms, several cell states coexist. For determining each cell type, cell–cell interactions are often essential, in addition to intracellular gene expression dynamics. Based on dynamical systems theory, we propose a mechanism for cell differentiation with regulation of populations of each cell type by taking simple cell models with gene expression dynamics. By incorporating several interaction kinetics, we found that the cell models with a single intracellular positive-feedback loop exhibit a cell fate switching, with a change in the total number of cells. The number of a given cell type or the population ratio of each cell type is preserved against the change in the total number of cells, depending on the form of cell–cell interaction. The differentiation is a result of bifurcation of cell states via the intercellular interactions, while the population regulation is explained by self-consistent determination of the bifurcation parameter through cell–cell interactions. The relevance of this mechanism to development and differentiation in several multicellular systems is discussed.

© 2008 Elsevier Ltd. All rights reserved.

1. Introduction

Complex gene regulatory or protein networks are responsible for determining cellular behaviors. The function of such networks has recently been discussed in the light of specific network structures called network motifs (Shen-Orr et al., 2002; Milo et al., 2002, 2004). Besides such motifs, several simple network modules are also considered to operate to give specific dynamical properties such as bistability, adaptation, or oscillatory behavior (Ferrell and Machleder, 1998; Sha et al., 2003; Tyson et al., 2003). Recent experimental results also suggest that such modules provide a basis for cell differentiation, as studied in competence state in *Bacillus subtilis* (Süel et al., 2006; Maamar et al., 2007).

In multicellular organisms, several cell states coexist. Morphogenesis with differentiation into distinct cell types, however, is not an event of independent single-cellular dynamics, but occurs as a result of an ensemble of interacting cells. For determining each cell type, cell–cell interactions are often essential besides intracellular dynamics by functional modules at a single cell level. In fact, gene regulatory networks responsible for the early developmental process or the cell specification process of several kinds of organisms include many intercellular interactions (Ben-Tabou de-Leon and Davidson, 2007; Davidson et al., 2002; Imai et al., 2006; Loose and Patient, 2004; Swiers et al., 2006).

The importance of cell–cell interactions to robust developmental processes is discussed as the community effect (Gurdon et al., 1993) and differentiation from equivalent groups of cells (Greenwald and Rubin, 1992).

When considering the development of a multicellular organism, not only a set of cell types, but also the number distribution of each of the cell types, has to be suitably determined and robust against perturbations during the course of development. The proportion of the body plan in planarian and in the slug of *Dictyostelium discoideum* is preserved over a wide range of body sizes (Oviedo et al., 2003; Ràfols et al., 2000). In the *D. discoideum* slug, the number ratio of two cell types is kept almost constant. In the hematopoietic system of mammals approximately 10 different cell types are generated from a hematopoietic stem cell, and their growth and differentiation are regulated to keep the number distribution of each cell to achieve homeostasis of the hematopoietic system. In this case, in addition to the proportion regulation, the absolute size of stem cell population is also important because all the hematopoietic cells will ultimately die out without their existence. Indeed, regulation of the numbers of each cell type is rather common in multicellular organisms. As the distribution of each cell type is a property of an ensemble of cells, cell–cell interactions should be essential for such regulation.

There are several theoretical studies discussing the importance of cell–cell interactions. By considering an ensemble of cells with intracellular genetic (or chemical) networks and intercellular interactions, synchronization of oscillation (García-Ojalvo et al., 2004; McMillen et al., 2002) or dynamical clusterings (Kaneko

* Corresponding author. Tel./fax: +81 3 5454 6732.

E-mail address: nakajima@complex.c.u-tokyo.ac.jp (A. Nakajima).

and Yomo, 1994, 1997; Mizuguchi and Sano, 1995; Furusawa and Kaneko, 1998; Ullner et al., 2007; Koseska et al., 2007) are observed. Cell states distinguishable from those of a single-cellular dynamics are generated, providing a basis for functional differentiation for multicellularity. The preservation of the proportion of different cell types is realized by taking advantage of Turing instability (Mizuguchi and Sano, 1995), while the robustness in the number distribution of different cell types is discovered in reaction network models (Kaneko and Yomo, 1994, 1999; Furusawa and Kaneko, 1998). Nevertheless, regulatory mechanisms for cell type populations are not elucidated in terms of dynamical systems because of the high dimensionality of the models.

In the present paper, we propose a regulatory mechanism of cell differentiation based on dynamical systems theory by taking simple cell models with biological gene regulation dynamics. Specifically, we study how cell states are differentiated with the change in the total cell number following cell–cell interactions. By incorporating different interaction kinetics, we show how simple functional modules generate specific cellular behaviors such as a cell fate switching, population size regulation of each cell type, and preservation of the number ratio of each cell type.

The present paper is organized as follows. In Section 2, we introduce an interacting multicellular model which is further analyzed in the present paper. Each cell has a simple functional module of genes, and its expression dynamics is modulated by the interactions with other cells. In Sections 3–5, we consider several different intercellular interactions, respectively. Although possible cell states are generated by an intracellular functional module, selection of one of these possible states or establishment of specific number distributions of cell states is realized depending on the manner of intercellular interactions. In Section 6, we extend our theoretical scheme to discuss the distribution of cell types in cell differentiation models studied so far (Kaneko and Yomo, 1997, 1999; Furusawa and Kaneko, 1998, 2001). Although these models have a complex intracellular reaction network, we show that the same logic can be applied to explain the cell differentiation observed in these models. In Section 7, we summarize our results and discuss their biological relevance and future directions.

2. Framework of the model

Here, we introduce a basic model of interacting cells with intracellular gene expression dynamics. Consider N cells with identical genes which interact through a common medium. The internal state of i -th cell is represented by the expression pattern of m genes, as $\vec{u}_i = (u_i^1, \dots, u_i^m)^T$. The medium under which cells are placed is represented by concentrations of n diffuse signals given by $\vec{v} = (v_1, \dots, v_n)^T$. As the simplest case, we discard the spatial configuration of cells so that each cell interacts with all the other cells via common signal chemicals \vec{v} . Each intracellular gene expression dynamics is modulated by these signal molecules, which give interactions with other cells.

For the sake of simplicity, we mostly examine the dynamics of single gene expression, in which the state of the i -th cell is expressed by only one variable, u_i , and the intercellular interaction is mediated by only one global diffusive signal, v . Considering an inhibitory effect of the intercellular interaction, u_i and v obey the following equation:

$$\begin{aligned} \frac{du_i(t)}{dt} &= f(u_i, v) \\ &= \frac{1}{\tau} \left(\frac{u_i^2(t)}{K_u^z + v^z(t) + u_i^z(t)} - u_i(t) + A_u \right) \end{aligned} \quad (1)$$

for $i = 1, \dots, N$,

$$\frac{dv(t)}{dt} = g(u_1, \dots, u_N, v). \quad (2)$$

Gene u_i activates its own expression through a feedback process, while the signal v has an inhibitory effect on the expression of the gene u_i . Although we adopt competitive inhibition here, the results to be discussed are qualitatively same even if other (anticompetitive or non-competitive) forms of inhibitory kinetics are chosen. Generally, the signal v is released by each cell depending on its gene expression level and the signal abundances at that moment. We adopt Hill-type kinetics for self-activation of the gene u_i . The parameter α denotes the Hill coefficient, i.e., the cooperativity of its kinetics, while K_u is the threshold for the activation of gene u_i in the absence of the signal v , and A_u is the activation rate of u_i by other molecules in the cell. The parameter τ is a time constant of the expression dynamics of u_i normalized by that of the signal v . In the present paper, we focus on the role of intercellular interaction on differentiation of cells in a population, so that the time scale of u_i is chosen to be much slower than that of v . This assumption on the time scale is rather natural biologically, as the gene expression occurs in a slower time scale. For numerical simulations, we use the following parameter values; $K_u = 0.1$, $A_u = 0.04$, $\alpha = 2.0$, and $\tau = 10.0$. In the present model parameter we study here, attractors of the system are always fixed points. Neither oscillatory nor more complex attractors exist. Note that the following results are qualitatively invariant as long as the Hill coefficient α is larger than unity.

Before studying the dynamics of a population of interacting cells, we first survey the single intracellular dynamics of Eq. (1) with v given as a constant control parameter. As is shown straightforwardly, the equation has a fixed point solution which exhibits two saddle-node bifurcations with the change in v (Fig. 1). We denote these bifurcation points as $v = v_1^*$ and $v = v_2^*$, and call the upper branch of the stable state as $u_{(1)}$ (or cell state 1) that is stable at $v \leq v_2^*$, and the other lower branch as $u_{(2)}$ (or cell state 2) that is stable at $v \geq v_1^*$. In the parameter region $v_1^* < v < v_2^*$, the bistability of $u_{(1)}$ and $u_{(2)}$ is observed.

As shown in Fig. 1, the only possible stationary states of each cell are $u_i = u_{(1)}$ or $u_i = u_{(2)}$. Depending on the value of v and also on the initial condition of u_i , each of the two solutions are selected. The question we address is as follows: how are these states selected and what determines a possible range in the number distribution of the two states when intercellular interactions through v are taken into account. In the following sections, we analyze three models with different types of the function

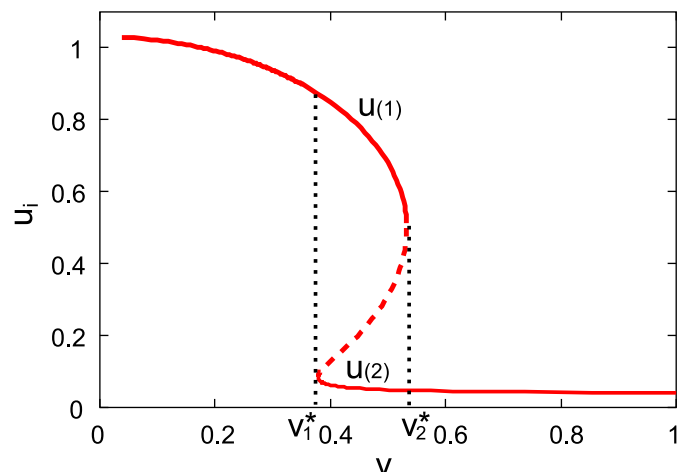


Fig. 1. The value u of the fixed point solution as a function of the signal concentration v in our model. Solid line indicates the stable solution, while the dotted line indicates the unstable one.

$g(u_1, \dots, u_N, v)$ to study how the differences in the kinetics of v lead to different types of regulation in the number distribution of cell types.

3. Model I: cell fate determination by total cell number

As a first example of interacting cells, we adopt a model in which each cell simply emits the signal v with the same rate. The kinetics of v obey the following equation:

$$\begin{aligned} \frac{dv(t)}{dt} &= g_1(u_1, \dots, u_N, v) \\ &= \sum_{i=1}^N c_i - v(t) = c_1 N - v(t), \end{aligned} \quad (3)$$

while the kinetics of $\{u_i\}$ obey Eq. (1). We are interested in the behavior of the stationary state as a function of the total cell number N . The stationary state solution of an ensemble of cells is generally obtained by the following procedure. First, we regard the signal v as a fixed parameter, not a variable, and obtain the solution u_i as a function of v , as already described in the previous section. Next, we write down v as a function of N and $\{u_i\}$ so that the self-consistent solution of the coupled equation is obtained, from which we analyze the dependence of the solution on the total cell number.

The stationary state is simply obtained by $du_i/dt = 0$ and $dv/dt = 0$. In the present case, the solution v is independent of $\{u_i\}$, and depends only on N , which leads to

$$f(u_i, v) = 0, \quad v = c_1 N. \quad (4)$$

The solution curve $f(u_i, v(N)) = 0$ is shown in Fig. 2, and the numerical result of the ratio of the number of each cell type to the total cell number is shown in Fig. 3. Here, we define a single cluster of an ensemble of cells as a state in which all the cells take the same stationary states, i.e.,

$$u_i = u_{(k)} \quad (k = 1 \text{ or } 2) \quad \text{for } i = 1, 2, \dots, N, \quad (5)$$

and a two-cluster state as that in which two cell types with $u = u_{(1)}$ and $u = u_{(2)}$ coexist, so that

$$u_i = \begin{cases} u_{(1)} & \text{for } i = 1, \dots, N_{(1)}, \\ u_{(2)} & \text{for } i = N_{(1)} + 1, \dots, N_{(1)} + N_{(2)} (= N). \end{cases} \quad (6)$$

Here, $N_{(1)}$ and $N_{(2)}$ denote the number of the cells with $u = u_{(1)}$ and $u = u_{(2)}$, respectively.

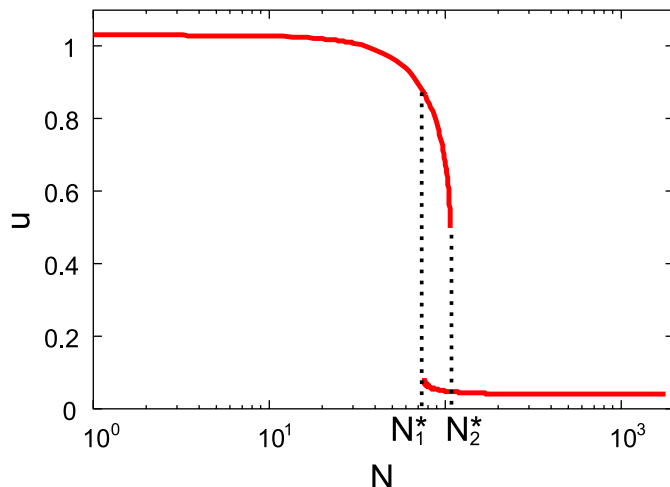


Fig. 2. The stationary states of u_i in model I are plotted against the total cell number N . At the interval $N_1^* \leq N \leq N_2^*$, two different cell states coexist. The parameter value c_1 is set at 0.005.

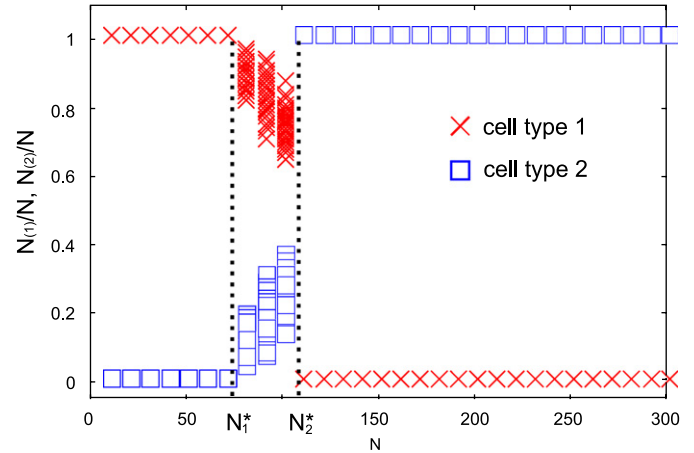


Fig. 3. The ratio of the number of each cell type (\times for $N_{(1)}$ and \square for $N_{(2)}$) plotted against the total cell number N , for model I. The initial values of u_i are chosen randomly from the interval of $u_i \in [0, 1]$. Data obtained from 100 different initial conditions are overlaid. The parameter value is $c_1 = 0.005$.

When the cell number N is lower than a threshold N_1^* ($= v_1^*/c_1$), the single-cluster state of $u_{(1)}$ is realized, while for N larger than a threshold N_2^* ($= v_2^*/c_1$), the single-cluster state of $u_{(2)}$ is realized, irrespectively of the initial cell state. Only within the range of $N_1^* \leq N \leq N_2^*$ are two-cluster states of $u_{(1)}$ and $u_{(2)}$ possible, where any population ratio of the cell types with $u_{(1)}$ to $u_{(2)}$ can be realized depending on the initial condition. Cell types switch between $u_{(1)}$ and $u_{(2)}$ simply by the total cell number, and the signal v works as a population size detector.

4. Model II: diversification from single state, and population size regulation of specific cell type

Next, we consider the case in which the signal induction depends on the expression level of u_i . We will show that the cells are differentiated into two types over a wide range of the total cell number N , and that the number of type 1 cells remains at a same level herein.

The kinetics of the signal v in model II is represented as follows:

$$\begin{aligned} \frac{dv(t)}{dt} &= g_2(u_1, \dots, u_N, v) \\ &= c_2 \sum_{i=1}^N \frac{u_i^\beta(t)}{K_v^\beta + u_i^\beta(t)} - v(t). \end{aligned} \quad (7)$$

Here we adopt Hill-type kinetics for the induction of the signal v by u_i , where β is the Hill coefficient, representing the cooperativity in the induction, and K_v denotes the threshold value for the signal induction. The parameter c_2 gives the maximum release rate of v from each cell.

Dependence of the stationary states on the total cell number is shown in Fig. 4. For a small N , all the cells always fall on a single-cluster state of $u_{(1)}$. As N gets larger, the bifurcation to a two-cluster state occurs, where the cells take either $u_{(1)}$ or $u_{(2)}$. Here, the single-cluster state of $u_{(1)}$ ($u_{(2)}$) is realized only at a small (large) number of cells, respectively, so that there is a gap in the total number of cells between the two single-cluster states. The two-cluster state exists within this gap.

To understand the observed dependence of the clustering behavior on the cell number, we first consider the stability of a single-cluster state. From $du_i/dt = 0$, $dv/dt = 0$, and $u_i = u_{(k)}$

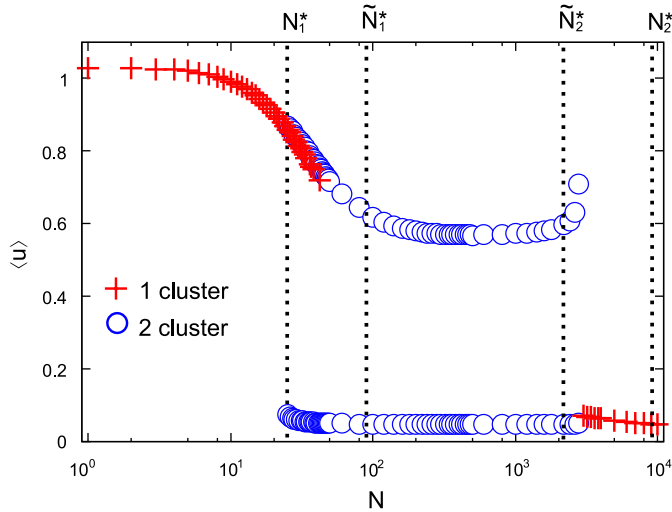


Fig. 4. The fixed point values of u_i in model II are plotted against the total cell number N . At each N , 100 initial conditions are chosen. The expression levels of u_i for a single-cluster (+) and two-cluster solutions (o) are plotted as a function of N . The value for two-cluster solutions is the average over initial conditions. The parameter values are set at $K_v = 2.0$, $\beta = 2.0$, and $c_2 = 0.1$.

($k = 1$ or 2) for $i = 1, \dots, N$, we get

$$f(u_{(k)}, v) = 0, \quad v = c_2 N \frac{u_{(k)}^\beta}{K_v^\beta + u_{(k)}^\beta}. \quad (8)$$

By solving the above equations self-consistently, the solution curve of u is obtained as a function of the total cell number N (Fig. 5). For $N < \tilde{N}_1^*$, a single-cluster state of $u_{(1)}$ is always stable. When the cell number increases beyond \tilde{N}_1^* , this single-cluster state becomes unstable, while for much larger N such that $N > \tilde{N}_2^*$, the single-cluster state becomes stable again, where the cell state is $u_{(2)}$ (Fig. 5). The thresholds \tilde{N}_1^* and \tilde{N}_2^* are given by $\tilde{N}_1^* = v_2^*(K_v^\beta + u_{(1)}^\beta(v_2^*)) / (c_2 u_{(1)}^\beta(v_2^*)) \simeq 92$ and $\tilde{N}_2^* = v_1^*(K_v^\beta + u_{(2)}^\beta(v_1^*)) / (c_2 u_{(2)}^\beta(v_1^*)) \simeq 2200$, respectively.

Next, consider the condition for the existence of a two-cluster state. Because the stability of a cell state is determined by the amount of v , the condition for the existence of a two-cluster state is given by $v_1^* < v < v_2^*$. Accordingly, considering v as a function of $N_{(1)}$ and N , a two-cluster state is possible if $N_{(1)}$ satisfies $v_1^* < v(N_{(1)}, N) < v_2^*$. Note that v satisfies $\partial v(N_{(1)}, N) / \partial N_{(1)} > 0$. Thus, the range of the cell number N in which a two-cluster state exists is given by $N_1^* < N < N_2^*$, where $N_1^* = v_1^*(K_v^\beta + u_{(1)}^\beta(v_1^*)) / (c_2 u_{(1)}^\beta(v_1^*)) \simeq 24$ and $N_2^* = v_2^*(K_v^\beta + u_{(2)}^\beta(v_2^*)) / (c_2 u_{(2)}^\beta(v_2^*)) \simeq 9400$, respectively. These threshold sizes satisfy $N_1^* < \tilde{N}_1^*$ and $\tilde{N}_2^* < N_2^*$, so that only two-cluster states are stable for N satisfying $\tilde{N}_1^* < N < \tilde{N}_2^*$. In the region satisfying $N_1^* < N < \tilde{N}_1^*$ and $\tilde{N}_2^* < N < N_2^*$, single-cluster and two-cluster states coexist, which is demonstrated in Fig. 4. In this case, either a single-cluster or two-cluster state is realized depending on the initial condition.

Because the number of each cell type in these two-cluster states has to satisfy the above condition, the range of possible numbers of two cell types is limited, depending on the total number of cells. The number of cell type 1 ($N_{(1)}$) from a variety of initial conditions is plotted as a function of N in Fig. 6. As N is increased beyond N_1^* , $N_{(1)}$ decreases linearly with N , with a rather small slope, over a wide range of N , up to \tilde{N}_2^* . Within this range the value of $N_{(1)}$ does not change so much.

To understand this behavior we obtain the dependency of $N_{(1)}$ on v and N . In a two-cluster state ($N_{(1)}, N_{(2)} (= N - N_{(1)})$), v is expressed by the contribution from the cell type 1 ($u_{(1)}(v)$) and

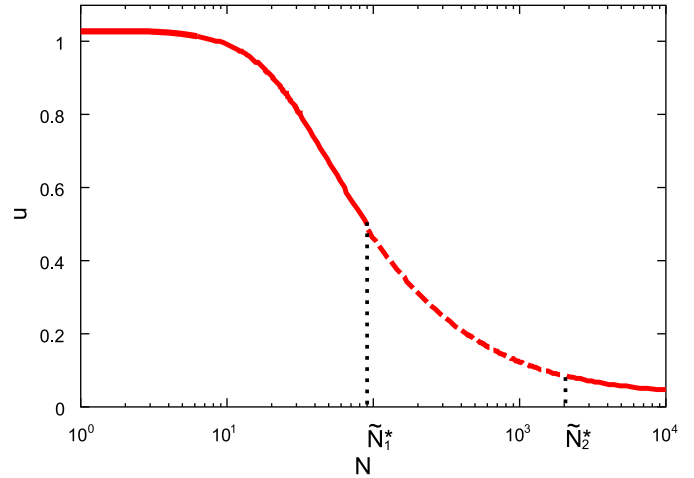


Fig. 5. The stationary state of a single-cluster solution for model II. Solid line indicates u_i of the stable fixed solution, while the broken line denotes that of the unstable one. The parameters are $K_v = 2.0$, $\beta = 2.0$, and $c_2 = 0.1$.

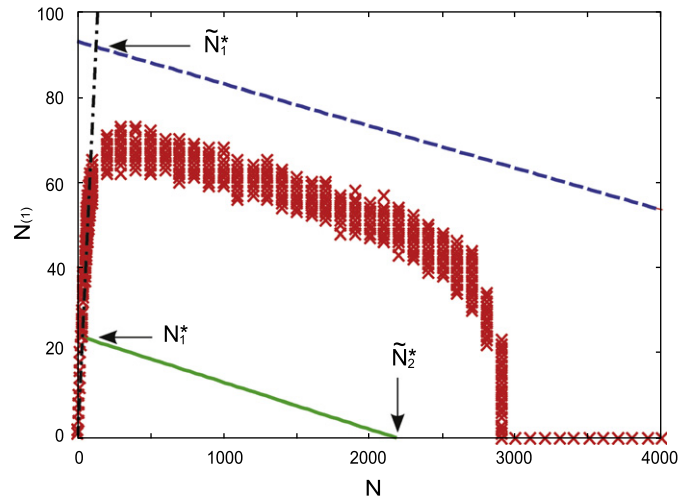


Fig. 6. The number of cell type 1 (\times) is plotted against the total cell number in model II. The initial condition of u_i is chosen randomly from the interval $u_i \in [0, 1]$. Solid and broken lines indicate $N_{(1)}(N, v_1^*) = -A(v_1^*)N + B(v_1^*)$ and $N_{(1)}(N, v_2^*) = -A(v_2^*)N + B(v_2^*)$, respectively, where $A(v_1^*) = 0.011$, $B(v_1^*) = 24$, $A(v_2^*) = 0.0099$, and $B(v_2^*) = 93$. The threshold values N_1^* , \tilde{N}_1^* , and \tilde{N}_2^* are indicated (N_2^* is out of the range of this figure). The parameters are $K_v = 2.0$, $\beta = 2.0$, and $c_2 = 0.1$.

type 2 ($u_{(2)}(v)$). By setting $du_i/dt = 0$, $dv/dt = 0$, and solving Eq. (7) for $N_{(1)}$, the number of type 1 cells $N_{(1)}$ is written as a function of N , given by

$$N_{(1)}(N, v) = -A(v)N + B(v) \quad (9)$$

with

$$A(v) = \frac{u_{(2)}^\beta(v) / (K_v^\beta + u_{(2)}^\beta(v))}{u_{(1)}^\beta(v) / (K_v^\beta + u_{(1)}^\beta(v)) - u_{(2)}^\beta(v) / (K_v^\beta + u_{(2)}^\beta(v))}, \quad (10)$$

$$B(v) = \frac{v}{c_2 \{u_{(1)}^\beta(v) / (K_v^\beta + u_{(1)}^\beta(v)) - u_{(2)}^\beta(v) / (K_v^\beta + u_{(2)}^\beta(v))\}}. \quad (11)$$

Here, we note that $u_{(1)}$ and $u_{(2)}$ are determined self-consistently as functions of v , and that $A(v) > 0$ and $B(v) > 0$. For the existence of a two-cluster state, v has to satisfy $v_1^* < v < v_2^*$, that is, $N_{(1)}(N, v_1^*) < N_{(1)}(N, v) < N_{(1)}(N, v_2^*)$ for each N . By inserting Eq. (9) into this expression, it is shown that $N_{(1)}(N, v_1^*)$ and $N_{(1)}(N, v_2^*)$, i.e., the lower and upper bounds of $N_{(1)}$, decay linearly with N , with

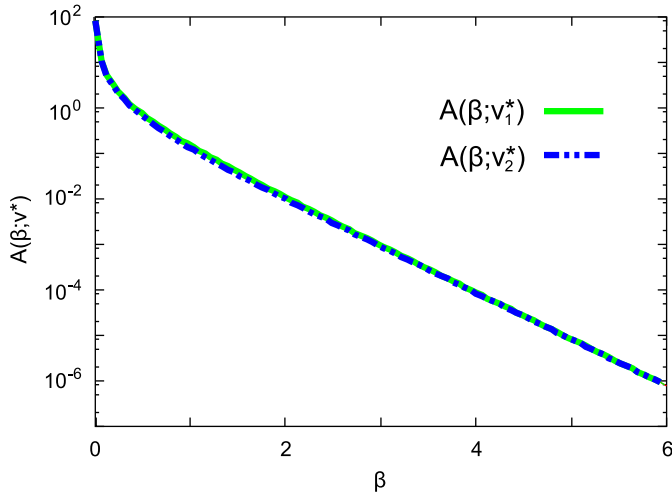


Fig. 7. The slope $A(\beta; v)$ is plotted as a function of β . Here, $A(\beta; v)$ for two different values of v , i.e., v_1^* and v_2^* are plotted, which agree within the resolution of the plot in the figure. The parameter values are $K_v = 2.0$, and $c_2 = 0.1$.

the slope of $A(v_1^*)$ and $A(v_2^*)$. In fact, a linear decrease in $N_{(1)}$ with the increase in N is clearly discernible in Fig. 6.

Next, we evaluate the value of the slope $A(v)$. Eq. (9) is written as $A(v) = \{(u_{(2)}/K_v)^\beta + (u_{(2)}/u_{(1)})^\beta\} / \{1 - (u_{(2)}/u_{(1)})^\beta\}$. If $u_{(2)} \ll u_{(1)}$ and $u_{(2)} \ll K_v$ are satisfied, that is the case for the parameters used in Fig. 6, $A(v)$ is much smaller than unity. As a result, the decrease in $N_{(1)}$ with N is slow, and $N_{(1)}$ is sustained at a same level over a wide range of N , satisfying $N_{(1)}(v_1^*) < N_{(1)}(v) < N_{(1)}(v_2^*)$ (Fig. 6).

By increasing the Hill coefficient β , $A(v)$ becomes much smaller than unity which asymptotically go to zero, even if the value of $u_{(2)}$ is the same level as $u_{(1)}$ or K_v as is shown in Fig. 7. Note that the conditions $u_{(2)} < u_{(1)}$ and $u_{(2)} < K_v$ have to be satisfied. The value of the slope $A(v)$ shows an exponential decrease with β . $A(v)^{-1}$ gives a measure for the range in which two-cluster states exist. Hence, $N_{(1)}$ is sustained at an almost constant level and the population size regulation of cell type 1 is realized with a sufficiently large β .

$$\tilde{B}(v) = \frac{v}{c_{v1} \{u_{(1)}^\beta(v) / (\tilde{K}_v^\beta + u_{(1)}^\beta(v)) - u_{(2)}^\beta(v) / (\tilde{K}_v^\beta + u_{(2)}^\beta(v))\} + c_{v2} \tilde{K}_v^\beta v \{1 / (\tilde{K}_v^\beta + u_{(2)}^\beta(v)) - 1 / (\tilde{K}_v^\beta + u_{(1)}^\beta(v))\}} \quad (15)$$

5. Model III: proportion preservation of two cell types

For precise body plan or for tissue homeostasis, proportion regulation of the number of each cell type is required. The fraction of each cell type has to be sustained at a certain range, against the change in the total number of cells. Here, we modify the kinetics of v in the previous model II to seek for the possibility of the proportion regulation. With this modification, we will show that the population fraction of the two types of cells is kept at a certain level against the change of N .

Here, the kinetics of v is modified as follows:

$$\frac{dv(t)}{dt} = g_3(u_1, \dots, u_N, v) = c_{v1} \sum_{i=1}^N \frac{u_i^\beta(t)}{\tilde{K}_v^\beta + u_i^\beta(t)} - c_{v2} v(t) \sum_{i=1}^N \frac{\tilde{K}_v^\beta}{\tilde{K}_v^\beta + u_i^\beta(t)} - v(t). \quad (12)$$

The modification to model II is just an addition of the second term in Eq. (12). In other words, each cell in this model also contributes to the degradation of the signal v .

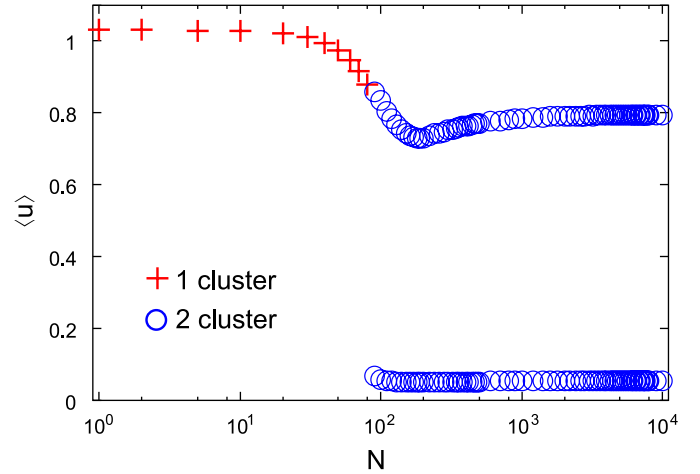


Fig. 8. The fixed point solutions of model III plotted against the total cell number N . At each N , 100 initial conditions are chosen. The expression levels of u_i for a single-cluster (+) and two-cluster solutions (o) are plotted as a function of N . The value for two-cluster solutions is the average over initial conditions. The parameter values are $\tilde{K}_v = 0.2$, $\beta = 2.0$, and $c_{v1} = c_{v2} = 0.005$.

As in the previous model, the cellular states fall on stationary states, and the bifurcation of the stationary state from a single-cluster to two-cluster states are observed with the increase in N (Fig. 8). Here, we first note that the two-cluster state remains stable over a wide range of N . Indeed, non-zero $N_{(1)}$ exists so that $v_1^* < v(N_{(1)}, N) < v_2^*$ is satisfied even for sufficiently large N .

Next, we study the population distribution of two cell types. As shown in Fig. 9, the ratio $N_{(1)}/N$ stays at a constant level against the change of N . In the same way as in the previous section, the dependency of $N_{(1)}$ on v and N for a two-cluster state is written as

$$\frac{N_{(1)}(N, v)}{N} = \tilde{A}(v) + \frac{\tilde{B}(v)}{N}, \quad (13)$$

$$\tilde{A}(v) = \left[1 + \frac{(c_{v1} u_{(1)}^\beta(v) - c_{v2} \tilde{K}_v^\beta v)}{(c_{v2} \tilde{K}_v^\beta v - c_{v1} u_{(2)}^\beta(v))} \left(\frac{\tilde{K}_v^\beta + u_{(2)}^\beta(v)}{\tilde{K}_v^\beta + u_{(1)}^\beta(v)} \right) \right]^{-1}, \quad (14)$$

$$\tilde{B}(v) = \frac{v}{c_{v1} \{u_{(1)}^\beta(v) / (\tilde{K}_v^\beta + u_{(1)}^\beta(v)) - u_{(2)}^\beta(v) / (\tilde{K}_v^\beta + u_{(2)}^\beta(v))\} + c_{v2} \tilde{K}_v^\beta v \{1 / (\tilde{K}_v^\beta + u_{(2)}^\beta(v)) - 1 / (\tilde{K}_v^\beta + u_{(1)}^\beta(v))\}} \quad (15)$$

Here, $\tilde{B}(v) > 0$ is always satisfied. Because v satisfies $v_1^* < v < v_2^*$ for the existence of a two-cluster state, $N_{(1)}/N$ is within the range $(\tilde{A}(v_1^*) + \tilde{B}(v_1^*)/N) < N_{(1)}(N, v)/N < (\tilde{A}(v_2^*) + \tilde{B}(v_2^*)/N)$ for each N . As a result, when N is sufficiently large, the possible range of $N_{(1)}/N$ is given by

$$\tilde{A}(v_1^*) < \frac{N_{(1)}}{N} < \tilde{A}(v_2^*). \quad (16)$$

From the above expression of $\tilde{A}(v)$, if the condition $(v_2^*/u_{(1)}^\beta(v_2^*)) < c_{v1}/(c_{v2} \tilde{K}_v^\beta) < (v_1^*/u_{(2)}^\beta(v_1^*))$ is satisfied, $\tilde{A}(v)$ is within $0 < \tilde{A}(v) < 1$. This is the case for the parameter values in Fig. 9. Thus, the cell type ratio of a two-cluster state has to be within the range given by Eq. (16), so that its ratio is insensitive to the change of the total number of cells. In addition, by increasing the Hill coefficient β , the range given by Eq. (16) gets narrower. Thus, the ratio $N_{(1)}/N$ is more accurately regulated. As β goes to infinity the range approaches its minimum, where the boundary is given by $\tilde{A}_\infty(v) = v/(c_{v1}/c_{v2} + v)$.

Note that $\tilde{A}(v)$ here is positive and is not necessarily small, in contrast to $A(v)$ in Eq. (9) for model II. Inclusion of the second term

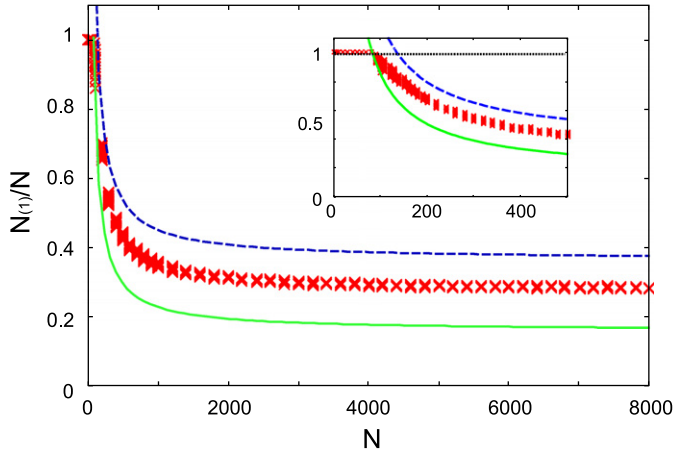


Fig. 9. The ratio of the number cell type 1 $N_{(1)}$ to the total cell number N is plotted against N for model III. The initial condition of u_i is chosen randomly from the interval of $u_i \in [0, 1]$. Solid and broken lines indicate $N_{(1)}(N, v_1^*)/N = \hat{A}(v_1^*) + \hat{B}(v_1^*)/N$ and $N_{(1)}(N, v_2^*)/N = \hat{A}(v_2^*) + \hat{B}(v_2^*)/N$, respectively, where $\hat{A}(v_1^*) = 0.16$, $\hat{B}(v_1^*) = 69$, $\hat{A}(v_2^*) = 0.36$, and $\hat{B}(v_2^*) = 86$. The parameter values are $\hat{K}_v = 0.2$, $\beta = 2.0$, and $c_{v1} = c_{v2} = 0.005$.

in Eq. (12) allows for this behavior, and the proportion regulation of cell types is achieved over a wide range of cells.

6. Cell differentiation model with random network

Here, we briefly discuss a general situation of cell differentiation models with intracellular dynamics and intercellular interactions with more genes (chemical species). As an example, we use the cell differentiation models of Kaneko–Yomo or Furusawa–Kaneko (Kaneko and Yomo, 1997, 1999; Furusawa and Kaneko, 1998, 2001). Here, we aim at demonstrating that the regulative behavior of cell differentiation in the previous sections generally works, which at the same time may provide a possible explanation for differentiation phenomena observed in their models. For the following analysis, we use one of the models (FK model) introduced in Furusawa and Kaneko (2001), while it is straightforwardly extended to other models.

In the FK model each cell has intracellular metabolic dynamics, and grows by uptake of the nutrients in the medium, and divides when the abundance of chemicals in the cell goes beyond a threshold. Accordingly, the total cell number N is also a time-dependent variable. As the cells share the same medium, they interact with other cells through uptake from the medium and exchange of chemicals with it.

The state of cell l is expressed by P different metabolites, $\vec{x}^{(l)} = (x_1^{(l)}, \dots, x_p^{(l)})^T$, and the nutrients are $\vec{X} = (X_1, \dots, X_Q)^T$, ($Q \leq P$). The dynamics of the i -th metabolite in cell l is given as follows:

$$\frac{dx_i^{(l)}(t)}{dt} = F_i(\{x_i^{(l)}(t)\}, X_i(t); \{C_{ijk}\}, \{\sigma_i\}), \quad (17)$$

A change in the concentration of the i -th nutrient in the medium with the volume V is given by

$$\frac{dX_i(t)}{dt} = D_{env}(S_i - X_i(t)) - \frac{D}{V} \sum_{m=1}^N (X_i(t) - x_i^{(m)}(t)). \quad (18)$$

S_i is the external source of the nutrient, D_{env} is the diffusion constant between the nutrient reservoir and the medium, and D is that across the cell membrane. Each cell grows through uptake of nutrients and changing them to other metabolites by Eq. (17). As the cells share the same medium, they interact with each other through competition for nutrients. Here, we confine our con-

sideration only to the behavior of nutrients $\{X_i\}$ in the stationary states for fixed N , and obtain the behavior of the stationary states as a function of N .

Because the stationary state satisfies the condition $dx_i^{(l)}/dt = 0$ and $dX_i/dt = 0$,

$$F_i(\{x_i^{(l)}\}, X_i; \{C_{ijk}\}, \{\sigma_i\}) = 0, \quad (19)$$

$$D_{env}(S_i - X_i) - \frac{D}{V} \sum_{m=1}^N (X_i - x_i^{(m)}) = 0. \quad (20)$$

From Eq. (19), possible stationary states of each cell, i.e., stationary solutions of $\vec{x}^{(l)}$, are obtained as a function of \vec{X} . Next, we describe how \vec{X} varies with N . As in the previous sections, we assume that the cell population takes an M -cluster state in the stationary state for a given N . By solving Eq. (20) for X_i , one obtains

$$X_i = \frac{\sum_{k=1}^M R_k \hat{x}_i^{(k)} + (VD_{env}/D)S_i/N}{1 + (VD_{env}/D)1/N}, \quad (21)$$

where $\hat{x}_i^{(k)}$ is the cell type k in an M -cluster state, and $R_k = N_k/N$, with N_k as the number of type k cells in the population. X_i is represented as a function of N and $\{R_k\}$. The stability condition of the M -cluster state of concern is expressed by N and $\{R_k\}$, from Eqs. (19) and (21). Thus, the realization of an M -cluster state depends on the number of cells or the ratio of cell types. Regulation of each cell type, as observed in Kaneko and Yomo (1997, 1999) and Furusawa and Kaneko (1998, 2001), is expected accordingly.

7. Summary and discussion

Through the analysis of several models, we see, (i) a switch of cell types via an increase in the total cell number, and (ii) diversification to two cell types. In addition, when the cells differentiate to two types, population size preservation of a specific cell type or proportion preservation of two cell types appears, depending on the interaction form with other cells. These behaviors are explained as a bifurcation of cell states via the intercellular interactions. First, possible cell types $u_{(1)}$ and $u_{(2)}$ are generated by a single positive-feedback loop, which works as a module for bistability. Secondly, intercellular signal v works as a bifurcation parameter, whose abundances determine the actual cell types. This bifurcation parameter is a function of the number of each cell type, depending on the intercellular interactions. Then, the resulting bifurcation parameter has to be determined self-consistently. This constraint restricts the number distribution of the cell types, which gives the mechanism of the regulation of the cell differentiation.

In model I, because the total cell number simply corresponds to the bifurcation parameter of cell states, the switch of the cell types by the total cell number is straightforward. In models II and III, since intercellular couplings change the bifurcation parameter, the transition from the single-cluster state of $u_{(1)}$ to a two-cluster state occurs by the increase in the total cell number. In model II, the cell type 2 contributes only weakly to the increase in v , compared with the cell type 1. Thus, the amount of v mainly depends on the number of the cell type 1. In contrast, in model III, the cell type 2 degrades v . As a result, the amount of v depends on the number ratio of two cell types.

If a gene expression network shows bistability with a bifurcation structure as in Fig. 1, cell differentiation is a general consequence when cell–cell couplings are introduced. An important point here is that the same intracellular module can be used in several different biological contexts by modifying only the intercellular interaction. This is quite useful in an evolutionary

perspective because new biological functions can be added by incorporating new interactions while preserving the intracellular core module.

Here, we discuss several phenomena in developmental biology that may be described by our models. First, we refer to two examples, the community effect and the mid-blastula transition, corresponding to model I. The community effect was discovered in muscle formation in reaggregated cells of the *Xenopus* embryo (Gurdon et al., 1993). Only when the number of cells is sufficiently large (i.e., more than 100), the cells differentiate to muscle. Cell–cell interaction, thus, is important for the differentiation, which is mediated by the diffusive factor eFGF, generated by each muscle progenitor cell (Standley et al., 2001; Fisher et al., 2002). The amount of eFGF increases with the total cell number, just like the signal v in model I. The precursor cells differentiate to non-muscle cells (correspond to cell type 1) if they are surrounded only by a small number of cells, while they differentiate to muscle cells (correspond to cell type 2) if they are surrounded by a large number of cells. The possible targets of the inhibition activity of eFGF are the transcription factors GATA-1 and GATA-2, the regulators of the erythropoiesis (Xu et al., 1999; Isaacs et al., 2007). In addition, eFGF can induce a transcription factor MyoD, the master regulator of myogenesis (Standley et al., 2001; Fisher et al., 2002). Thus, the differentiation decision between erythropoiesis and myogenesis by eFGF is dependent on the cell number, as in our model I.

Another example of model I may be given by mid-blastula transition. In the cell cycle machinery in *Xenopus*, the phosphorylation states of the cyclin dependent kinase Cdc2 have a fundamental role in the entry into mitosis (Hartley et al., 1996; Nigg, 2001). Cdc2 positively regulates its own active state via an activation of the phosphatase Cdc25 and via an inhibition of the kinase Wee1. As opposed to the positive feedback of Cdc2, the kinase Chk1 inhibits Cdc25 and activates Wee1, and thus inactivates Cdc2. Hence it is possible that the amount of active Cdc2 shows bistability depending on the amount of active Chk1 (Novak and Tyson, 1993). Here, DNA accelerates the phosphorylation of Chk1 and activates Chk1. Thus, the increase in DNA amount via cleavage in the early embryo can induce a transition from the active to inactive state of Cdc2. This transition is considered to trigger the mid-blastula transition in *Xenopus* (Novak and Tyson, 1993; Shimuta et al., 2002; Peng et al., 2007). This induced change can fit well with the transition observed in model I, in the sense that the system parameter (the concentration of the signal v in our model or the amount of active Chk1 in the mid-blastula transition) changes as a function of the cell number, which induces a transition of the cell state. To be precise, the bifurcation parameter in the mid-blastula transition refers to the DNA content instead of the cell number. Also, we should mention that mid-blastula transition involves many other factors such as the change in cell motility and the initiation of zygotic gene transcriptions (Yasuda and Schubiger, 1992), which are not included in the present study. Still, the core part of the transition could be described by our mechanism.

It is known that mid-blastula transition occurs when the ratio of DNA to cytoplasm in each individual cell is increased beyond a threshold (Newport and Kirschner, 1982a, b). In our model I, the transition threshold is v_2^* , which is equal to cN_2^* . The parameter c corresponds to the inverse of the amount of a cytoplasmic factor which has an inhibitory effect to Chk1 or has a competitive effect on DNA. Then, addition (depletion) of cytosol to an egg in the experiment corresponds to decrease (increase) in the parameter value of c in model. Thus, also in model I, the threshold for the transition is determined by the ratio of the DNA amount N to a cytoplasmic factor c^{-1} . Before the mid-blastula transition, however, the amount of cytoplasm shows only little change, and thus

the parameter c^{-1} is almost constant. Therefore, the DNA amount works as the bifurcation parameter for the mid-blastula transition.

Secondly, as for model II, consider the maintenance of the hematopoietic stem cells in mammals. Here, the transcription factor GATA-2 is known to play an essential role for the maintenance of hematopoietic stem cell and hematopoietic progenitors (Cantor and Orkin, 2002; Swiers et al., 2006). GATA-2 expression is active in hematopoietic stem cell, while during erythropoiesis, it is switched off, and is replaced by the active expression of the transcription factor GATA-1. GATA-2 activates itself and maintains its expression once activated, while GATA-1 suppresses GATA-2 transcription with FOG-1.

Generally, an environment called stem cell niche is needed for the maintenance of the stem cell population. In a hematopoietic system, osteoblasts are known to work as such stem cell niche (Calvi, 2006). The stem cells compete for some chemical factors derived from this niche, and the cells which cannot take the factors differentiate to specific hematopoietic lineages. Indeed, the competition for these factors has been discussed to be essential to the regulation of the stem cell population size, while competence for these factors decrease through the differentiation process (Radtke et al., 2004). In fact, several factors such as Angiopoietin-1, Wnt, Notch-ligand Jagged1 are identified as mediators for this niche-stem interaction (Arai et al., 2004; Adams and Scadden, 2006; Rattis et al., 2004). For example, Notch signals inhibit the erythroid differentiation by suppressing GATA-1 activity through Hes1 (Ishiko et al., 2005; Kunisato et al., 2003). Hence, it is possible that GATA-2/GATA-1 transition is regulated by the degree of the GATA-1 mediated repression of GATA-2 which is modulated by Notch (Swiers et al., 2006). Once several cells of the stem cell population differentiate, the differentiated cells cannot respond to Jagged1 because of the decrease in the expression of Notch (Radtke et al., 2004). The competition for the niche is then relaxed, so that a certain fraction of undifferentiated cells remained as stem cells stably.

To sum up, the strength of GATA-2 repression increases with the increase in the number of hematopoietic stem cells. Through this change, the erythroid differentiation is induced and the number of stem cells is maintained at a certain level. Following this discussion, we propose that this process is described by assigning GATA-2 and Notch-ligand Jagged1 as the chemical u_i and v in our model II, respectively. If this assignment is correct, GATA-2 expression is expected to show bistability for a certain range of Jagged1 stimulation. By examining this theoretical prediction experimentally, it will be possible to confirm the validity of the application of our model to the hematopoietic stem cell system. Here, we should mention that, the above example for Notch often assumes the spatial heterogeneity implicitly. Even though the spatial heterogeneity was not included in our model here, extension to include it is rather straightforward, which does not alter the conclusion here. Recently, it is shown that Wnt uses the same signaling pathway as Notch for the maintenance of hematopoietic stem cells and that Wnt signal upregulates Hes1 (Duncan et al., 2005; Espinosa et al., 2003). Hence it is possible that GATA-2/GATA-1 transition is also regulated via Wnt signal.

Thirdly, our model III may be applied to the proportion regulation of prestalk-cell types and prespore-cell types in the *Dictyostelium* slug. Differentiation to prespore cells is induced by cAMP, and the cell state is maintained by a positive-feedback loop of prespore cell specific adenylyl cyclase G activity (Hopper et al., 1993; Williams, 2006; Alvarez-Curto et al., 2007). On the other hand, differentiation-inducing factor-1 (DIF-1) is necessary for the differentiation from a prespore-cell to a prestalk-cell (at least for the differentiation to pstO, which is a subtype of the prestalk-cell)

(Williams, 2006; Kay and Thompson, 2001). As an intercellular interaction, this DIF-1 is produced by prespore-cells, and are degraded by prestalk-cells. This cell-type specific induction/destruction of DIF-1 is responsible for the proportion preservation as studied in model III.

Of course, the present multicellular organisms also adopt other mechanisms of differentiation such as morphogen gradient (Freeman and Gurdon, 2002; Tabata and Takei, 2004), besides the intracellular–intercellular dynamical mechanism discussed here. How the both mechanisms are used cooperatively will be important for understanding the development of present multicellular organisms. On the other hand, since the mechanism discussed here requires neither external morphogen gradient nor detailed gene expression network with finely tuned parameters, it is natural to expect that it worked at an evolutionarily ancient stage in multicellular development, whereas sophisticated mechanisms as in the present organisms are evolved later (Forgacs and Newman, 2005). The intracellular–intercellular dynamical mechanism here requires just a few chemicals, and is easily accessible. More sophisticated mechanisms of differentiation, using prepattern of morphogen gradient and/or using well designed genetic network, could be evolved later to achieve more complex architecture of body plan with robust and fast developmental process.

Based on our model, we can consider a possible scenario for evolution of cell differentiation in multicellular organisms. Since bistability can provide a memory in a cell system, it would also be beneficial to unicellular organisms as a phenotypic switch to respond environmental stimulus. Hence, unicellular systems might attain bistability before evolution to multicellularity. When these cells emit some chemical factors to which they respond and communicate, interacting cells begin to show some kind of differentiation as shown in the present paper. Indeed bacteria in a biofilm take different cell states from a free living cell, which may represent ancient type of cell differentiation (Davies et al., 1998). It is interesting to seek the origin of multicellularity along this line (Furusawa and Kaneko, 2002) both theoretically and experimentally.

Although we confine our analysis to a system with only fixed point solutions, oscillatory and other dynamical behaviors are often observed in biological systems. The analysis we introduced here is also applicable to such cases, as long as there are bifurcations of attractors with the change in relevant chemical concentrations which are influenced by cell–cell interactions. On the other hand, oscillatory behaviors may bring about richer bifurcations, as well as clustering of cells with regards to the oscillation phase or amplitude, as has been discussed in models with intracellular oscillatory dynamics and cell–cell interactions (Kaneko and Yomo, 1994, 1997; Koseska et al., 2007; Ullner et al., 2007). The study of possible forms on differentiations and regulations in such dynamical systems will be important in future. In multicellular systems, cells behave in coordination by taking advantage of communication with other cells. Such collective behavior is a result of interacting systems with intracellular gene expression dynamics. The present self-consistent determination of bifurcation parameters through cell–cell interactions will be essential to understand organization in multicellularity.

8. Method

Computer programs for the simulation of each model are written in C language, and are compiled with gcc version 4.1.2. Standard 4th order Runge–Kutta method is used for numerical integration.

Acknowledgments

The authors would like to thank M. Tachikawa, N. Kataoka, K. Fujimoto for stimulating discussions, and S. Ishihara for discussions and reading the manuscript.

References

- Adams, G.B., Scadden, D.T., 2006. The hematopoietic stem cell in its place. *Nat. Immunol.* 7, 333–337.
- Alvarez-Curto, E., Saran, S., Meima, M., Zobel, J., Scott, C., Schaap, P., 2007. cAMP production by adenylyl cyclase G induces prespore differentiation in *Dictyostelium* slugs. *Development* 134, 959–966.
- Arai, F., Hirao, A., Ohmura, M., Sato, H., Matsuoka, S., Takubo, K., Ito, K., Koh, G.Y., Suda, T., 2004. Tie2/Angiopoietin-1 signaling regulates hematopoietic stem cell quiescence in the bone marrow niche. *Cell* 118, 149–161.
- Ben-Tabou de-Leon, S., Davidson, E.H., 2007. Gene regulation: gene control network in development. *Annu. Rev. Biophys. Biomol. Struct.* 36, 191–212.
- Calvi, L.M., 2006. Osteoblastic activation in the hematopoietic stem cell niche. *Ann. N.Y. Acad. Sci.* 1068, 477–488.
- Cantor, A.B., Orkin, S.H., 2002. Transcriptional regulation of erythropoiesis: an affair involving multiple partners. *Oncogene* 21, 3368–3376.
- Davidson, E.H., et al., 2002. A genomic regulatory network for development. *Science* 295, 1669–1678.
- Davies, D.G., Parsek, M.R., Pearson, J.P., Iglewski, B.H., Costerton, J.W., Greenberger, E.P., 1998. The involvement of cell-to-cell signals in the development of a bacterial biofilm. *Science* 280, 295–298.
- Duncan, A.W., Rattis, F.M., DiMascio, L.N., Congdon, K.L., Pazianos, G., Zhao, C., Yoon, K., Cook, J.M., Willert, K., Gaiano, N., Reya, T., 2005. Integration of Notch and Wnt signaling in hematopoietic stem cell maintenance. *Nat. Immunol.* 6, 314–322.
- Espinosa, L., Inglés-Esteve, J., Aguilera, C., Bigas, A., 2003. Phosphorylation by glycogen synthase kinase-3 β down-regulates notch activity, a link for Notch and Wnt pathways. 2003. *J. Biol. Chem.* 278, 32227–32235.
- Ferrell Jr., J.E., Machleder, E.M., 1998. The biochemical basis of an all-or-none cell fate switch in *Xenopus oocytes*. *Science* 280, 895–898.
- Fisher, M.E., Isaacs, H.V., Pownall, M.E., 2002. eFGF is required for activation of XmyoD expression in the myogenic cell lineage of *Xenopus laevis*. *Development* 129, 1307–1315.
- Forgacs, G., Newman, S.A., 2005. *Biological Physics of the Developing Embryo*. Cambridge University Press, Cambridge.
- Freeman, M., Gurdon, J.B., 2002. Regulatory principles of developmental signaling. *Annu. Rev. Cell Dev. Biol.* 18, 515–539.
- Furusawa, C., Kaneko, K., 1998. Emergence of rules in cell society: differentiation, hierarchy, and stability. *Bull. Math. Biol.* 60, 659–687.
- Furusawa, C., Kaneko, K., 2001. Theory of robustness of irreversible differentiation in a stem cell system: chaos hypothesis. *J. Theor. Biol.* 209, 395–416.
- Furusawa, C., Kaneko, K., 2002. Origin of multicellular organisms as an inevitable consequence of dynamical systems. *Anat. Rec.* 268, 327–342.
- García-Ojalvo, J., Elowitz, M.B., Strogatz, S.H., 2004. Modeling a synthetic multi-cellular clock: repressilators coupled by quorum sensing. *Proc. Natl. Acad. Sci. USA* 101, 10955–10960.
- Greenwald, I., Rubin, G.M., 1992. Making a difference: the role of cell–cell interactions in establishing separate identities for equivalent cells. *Cell* 68, 271–281.
- Gurdon, J.B., Lemaire, P., Kato, K., 1993. Community effects and related phenomena in development. *Cell* 75, 831–834.
- Hartley, R.S., Rempel, R.E., Maller, J.L., 1996. In vivo regulation of the early embryonic cell cycle in *Xenopus*. *Dev. Biol.* 173, 408–419.
- Hopper, N.A., Harwood, A.J., Bouzid, S., Véron, M., Williams, J.G., 1993. Activation of the prespore and spore cell pathway of *Dictyostelium* differentiation by cAMP-dependent protein kinase and evidence for its upstream regulation by ammonia. *EMBO J.* 12, 2459–2466.
- Imai, K.S., Levine, M., Satoh, N., Satou, Y., 2006. Regulatory blueprint for a chordate embryo. *Science* 312, 1183–1187.
- Isaacs, H.V., Deconinck, A.E., EPownall, M., 2007. FGF4 regulates blood and muscle specification in *Xenopus laevis*. *Biol. Cell* 99, 165–173.
- Ishiko, E., Matsumura, I., Ezoe, S., Gale, K., Ishiko, J., Satoh, Y., Tanaka, H., Shibayama, H., Mizuki, M., Era, T., Enver, T., Kanakura, Y., 2005. Notch signals inhibit the development of erythroid/megakaryocytic cells by suppressing GATA-1 activity through the induction of HES1. *J. Biol. Chem.* 280, 4929–4939.
- Kaneko, K., Yomo, T., 1994. Cell division differentiation and dynamic clustering. *Physica D* 75, 89–102.
- Kaneko, K., Yomo, T., 1997. Isologous diversification: a theory of cell differentiation. *Bull. Math. Biol.* 59, 139–196.
- Kaneko, K., Yomo, T., 1999. Isologous diversification for robust development of cell society. *J. Theor. Biol.* 199, 243–256.
- Kay, R.R., Thompson, C.R.L., 2001. Cross-induction of cell types in *Dictyostelium*: evidence that DIF-1 is made by prespore cells. *Development* 128, 4959–4966.
- Koseska, A., Volkov, E., Zaikin, A., Kurths, J., 2007. Inherent multistability in arrays of autoinducer coupled genetic oscillators. *Phys. Rev. E* 75, 031916.
- Kunisato, A., Chiba, S., Nakagami-Yamaguchi, E., Kumano, K., Saito, T., Masuda, S., Yamaguchi, T., Osawa, M., Kageyama, R., Nakauchi, H., Nishikawa, M., Hirai, H.,

2003. HES-1 preserves purified hematopoietic stem cells ex vivo and accumulates side population cells in vivo. *Blood* 101, 1777–1783.
- Loose, M., Patient, R., 2004. A genetic regulatory network for *Xenopus mesendoderm* formation. *Dev. Biol.* 271, 467–478.
- Maamar, H., Raj, A., Dubnau, D., 2007. Noise in gene expression determines cell fate in *Bacillus subtilis*. *Science* 317, 526–529.
- McMillen, D., Kopell, N., Hasty, J., Collins, J.J., 2002. Synchronizing genetic relaxation oscillators by intercell signaling. *Proc. Natl. Acad. Sci. USA* 99, 679–684.
- Milo, R., Shen-Orr, S., Itzkovitz, S., Kashtan, N., Chklovskii, D., Alon, U., 2002. Network motifs: simple building blocks of complex networks. *Science* 298, 824–827.
- Milo, R., Itzkovitz, S., Kashtan, N., Levitt, R., Shen-Orr, S., Ayzenshtat, I., Sheffer, M., Alon, U., 2004. Superfamilies of evolved and designed networks. *Science* 303, 1538–1542.
- Mizuguchi, T., Sano, M., 1995. Proportion regulation of biological cells in globally coupled nonlinear systems. *Phys. Rev. Lett.* 75, 966–969.
- Newport, J., Kirschner, M., 1982a. A major developmental transition in early *Xenopus* embryos: I. Characterization and timing of cellular changes at the midblastula stage. *Cell* 30, 675–686.
- Newport, J., Kirschner, M., 1982b. A major developmental transition in early *Xenopus* embryos: II. Control of the onset of transcription. *Cell* 30, 687–696.
- Nigg, E.A., 2001. Mitotic kinases as regulators of cell division and its checkpoints. *Nat. Rev. Mol. Cell Biol.* 2, 21–32.
- Novak, B., Tyson, J.J., 1993. Numerical analysis of a comprehensive model of m-phase control in *Xenopus oocyte* extracts and intact embryos. *J. Cell Sci.* 106, 1153–1168.
- Oviedo, N.J., Newmark, P.A., Alvarado, A.S., 2003. Allometric scaling and proportion regulation in the freshwater planarian *Schmidtea mediterranea*. *Dev. Dyn.* 226, 326–333.
- Peng, A., Lewellyn, A.L., Maller, J.L., 2007. Undamaged DNA transmits and enhances DNA damage checkpoint signals in early embryos. *Mol. Cell Biol.* 27, 6852–6862.
- Radtke, F., Wilson, A., Mancini, S.J.C., MacDonald, R., 2004. Notch regulation of lymphocyte development and function. *Nat. Immunol.* 5, 247–253.
- Ràfols, I., Amagai, A., Maeda, Y., MacWilliams, H.K., Sawada, Y., 2000. Cell type proportioning in Dictyostelium slugs: lack of regulation within a 2.5-fold tolerance range. *Differentiation* 67, 107–116.
- Rattis, F.M., Voermans, C., Reya, T., 2004. Wnt signaling in the stem cell niche. *Curr. Opin. Hematol.* 11, 88–94.
- Sha, W., Moore, J., Chen, K., Lassaletta, A.D., Chung-Seon Yi, J.J.T., Sible, J.C., 2003. Hysteresis drives cell-cycle transitions in *Xenopus laevis* egg extracts. *Proc. Natl. Acad. Sci. USA* 100, 975–980.
- Shen-Orr, S.S., Milo, R., Mangan, S., Alon, U., 2002. Network motifs in the transcriptional regulation network of *Escherichia coli*. *Nat. Gen.* 31, 64–68.
- Shimuta, K., Nakajo, N., Uto, K., Hayano, Y., Okazaki, K., Sagata, N., 2002. Chk1 is activated transiently and targets Cdc25A for degradation at the *Xenopus* midblastula transition. *EMBO J.* 21, 3694–3703.
- Standley, H.J., Zorn, A.M., Gurdon, J.B., 2001. eFGF and its mode of action in the community effect during *Xenopus* myogenesis. *Development* 128, 1347–1357.
- Süel, G.M., García-Ojalvo, J., Liberman, L.M., Elowitz, M.B., 2006. An excitable gene regulatory circuit induces transient cellular differentiation. *Nature* 440, 545–550.
- Swiers, G., Patient, R., Loose, M., 2006. Genetic regulatory networks programming hematopoietic stem cells and erythroid lineage specification. *Dev. Biol.* 294, 525–540.
- Tabata, T., Takei, Y., 2004. Morphogens, their identification and regulation. *Development* 131, 703–712.
- Tyson, J.J., Chen, K.C., Novak, B., 2003. Sniffers, buzzers, toggles and blinkers: dynamics of regulatory and signaling pathways in the cell. *Curr. Opin.* 15, 221–231.
- Ullner, E., Zaikin, A., Volkov, E.I., García-Ojalvo, J., 2007. Multistability and clustering in a population of synthetic genetic oscillators via phase-repulsive cell-to-cell communication. *Phys. Rev. Lett.* 99, 148103.
- Williams, J.G., 2006. Transcriptional regulation of Dictyostelium pattern formation. *EMBO Rep.* 7, 694–698.
- Xu, R.H., Ault, K.T., Kim, J., Park, M.J., Hwang, Y.S., Peng, Y., Sredni, D., Kung, H.F., 1999. Opposite effects of FGF and BMP-4 on embryonic blood formation: roles of PV.1 and GATA-2. *Dev. Biol.* 208, 352–361.
- Yasuda, G.K., Schubiger, G., 1992. Temporal regulation in the early embryo: is MBT too good to be true. *Trends Genet.* 8, 124–127.